



## Original article

# Multi-response optimization and neural network modeling for parameter precision in heat reflux extraction of spice oleoresins from two pepper cultivars (*Piper nigrum*)



Olusegun Abayomi Olalere\*, Nour Hamid Abdurahman, Rosli bin Mohd Yunus, Oluwaseun Ruth Alara

Faculty of Chemical & Natural Resources Engineering, Universiti Malaysia Pahang, Lebuhraya Tun Razak, 26300 Gambang, Pahang, Malaysia

## ARTICLE INFO

## Article history:

Received 2 August 2017

Accepted 12 September 2017

Available online 18 September 2017

## Keywords:

Artificial neural network  
Black and white pepper  
Gas Chromatography-Mass Spectrometry (GC-MS) analysis  
Multi-response optimization  
Taguchi method

## ABSTRACT

Black and white peppers are important oil bearing commodity crop in tropical areas. They are highly beneficial in food industries and herbal medicine, due to their amazing aroma and therapeutic activities. In this study, heat reflux technique was employed to extract medicinal oleoresin from the two peppercorns. For this purpose, various extraction parameters were considered viz: extraction time, particle size and feed-solvent ratio. These extraction parameters were employed to optimize the extraction yield and absorbed energy via Taguchi methodology. The established optimal condition values of the yield and absorbed energy from the parametric study were 13.22 mg/g and 285.60 J/min, respectively in black pepper heat refluxation. Moreover, in white pepper refluxation, the extraction yield and absorbed energy were 14.04 mg/g and 264.82 J/min, respectively. Artificial neural network (ANN) was used for prediction purposes. This was achieved by comparing two algorithms, transfer functions and neurons. A good training and better prediction of the experimental data were observed using the Levenberg Marquardt (LM) feed forward backpropagation algorithm with log sigmoid transfer function as hidden layer and 3-4-5-1 as model topology. Furthermore, a total of 19 and 25 bioactive compounds were identified in black and white pepper extracts, respectively. The results from the Scanning Electron Spectrometry (SEM) showed a remarkable morphological changes during the heat refluxation process.

© 2017 The Authors. Production and hosting by Elsevier B.V. on behalf of King Saud University. This is an open access article under the CC BY-NC-ND license (<http://creativecommons.org/licenses/by-nc-nd/4.0/>).

## 1. Introduction

Black and white peppers are important perennial aromatic and oil bearing industrial crops grown in the tropical area (Shahida et al., 2013). They are woody climbing plant which belong to the genus *Piper nigrum* L and *Piperaceae* family respectively (Scott et al., 2007). They are functional commodity crops with both nutritional and medicinal properties. The two pepper cultivars are the world most used spices, extensively applied in food industries as spices; due to their amazing aroma and characteristic pungency. A recent study has therefore shown their efficacy as carminative, anti-inflammatory, anti-cold, anti-bacterial and bioavailable

agents for the treatment of many degenerative diseases (Jagella and Grosch, 1999; Olalere et al., 2017; Reshmi et al., 2010). The extraction of a complete bioactive extracts which doubled as massage oil for aromatherapy, and as bioavailability enhancer in the assimilation of other drugs, is the focus of this research (Abdurahman and Olalere, 2016; Janakiraman and Manavalan, 2008). The hydrodistillation method is an important techniques which had been previously used in extracting oil from black and white pepper (Abdurahman and Olalere, 2016; Gavahian et al., 2015; Mohan et al., 2013; Raman and Gaikar, 2002). However, the extraction of complete oleoresin oil requires a special experimental set-up consisting of reflux configuration. This resulted in a novel heat reflux technique which differs in configuration from hydrodistillation extraction process due to the introduction of a reflux condenser, which functions for both the cooling and condensation of bioactive compounds. This configuration has an advantage of preventing overheating, which could result in bumping phenomenon and an eventual variation in the quality of the extracted oleoresin.

In recent times, the neural network model has been a versatile tool for intelligent prediction of a wide range of chemical and

\* Corresponding author.

E-mail address: [olabayor@gmail.com](mailto:olabayor@gmail.com) (O.A. Olalere).

Peer review under responsibility of King Saud University.



Production and hosting by Elsevier

physical applications such as in bio-fuel production (Betiku and Taiwo, 2015) and manufacturing process (Adedeji et al., 2014). It has also been successfully used for natural product extraction processes (Sahin et al., 2017; Şahin et al., 2017; Toboc and Lavric, 2012). The main objective of this research is to investigate the effects of three operating parameters using a multi-response optimization and artificial neural network modelling for optimized extraction yield and energy intensification.

## 2. Materials and methods

### 2.1. Materials

The standard grade dried black (4% moisture) and white peppers were bought from Malaysian Pepper Board (MPB) in Sarawak. The samples were then pulverized into powdery form using a Knife Mill Grindomix grinder (GM-200 model, Germany). The powdered samples were thereafter sieved into five different homogenous particle sizes (0.105 mm, 0.154 mm, 0.300 mm, 0.450 mm and 0.900 mm) and preserved in an airtight plastic.

### 2.2. Extraction of fixed oil through heat reflux technique

An accurately weighed pepper sample (25 g) was loaded into a 1 L volumetric flask containing distilled water with the method used by Mohan et al. (2013). The sample was then filtered and concentrated using rotary evaporator (BUCHI, R-200 model, Germany). The extraction yield was calculated on the dry basis and stored at 4 °C in a dark vial prior to further analysis.

### 2.3. Determination of specific energy absorbed

The energy absorbed by the system is an important variable to measure during the extraction process. A proper energy audit of the heat reflux system requires a balance between the total energy emitted and the energy absorbed by the water-sample. In this study, the energy absorbed by the water-pepper system consisted of the energy required in vaporizing the solvent plus the energy required for actual extraction as presented in the following sets of heat balance equations (Eqs. (1)(3)):

$$Q_t = \frac{Q_v + Q_s}{t} \quad (1)$$

$$Q_v = h_{fg}(w_f - w_i) \quad (2)$$

$$Q_s = \rho V C_p (T_f - T_i) \quad (3)$$

where  $Q_t$  = total absorbed energy,  $Q_v$  = energy required in vaporizing the solvent,  $Q_s$  = sensible energy, required for actual extraction,  $\rho$  = Density of extracting solvent ( $\text{gcm}^{-3}$ ),  $V$  = Volume of extracting ( $\text{cm}^3$ ),  $C_p$  = Specific heat capacity of extracting solvent ( $\text{Jg}^{-1}\text{C}^{-1}$ ),  $h_{fg}$  = Latent heat of extracting solvent ( $\text{Jg}^{-1}$ ),  $T_i$  = Pre-heating pulsed temperature ( $^{\circ}\text{C}$ ),  $T_f$  = Irradiation temperature ( $^{\circ}\text{C}$ ),  $\Delta w$  = Solvent dissipated ( $\text{cm}^{-3}$ ),  $w_i$  = Initial weight of solvent before extraction (g),  $w_f$  = Initial weight of solvent before extraction (g),  $t$  = irradiation time (mins).

## 2.4. Modeling and optimization studies

### 2.4.1. Taguchi experimental design

Design of experiments (DOE) was adopted for the parametric optimization of three extraction parameters via MINITAB 17<sup>®</sup> (Minitab Inc., PA, U.S.A.) (Mandal et al., 2008; Thakker et al., 2016). The extraction parameters used for this study were, extrac-

**Table 1**  
Extraction factors and levels.

Levels	Black pepper heat reflux			White pepper heat reflux		
	A (min)	B (mm)	C	A (min)	B (mm)	C
$\beta_1$	120	0.105	1:14	120	0.105	1:14
$\beta_2$	180	0.154	1:16	180	0.154	1:16
$\beta_3$	240	0.300	1:18	240	0.300	1:18

tions time (A), particle size (B) and feed-solvent ratio (C). The saturation  $L_9$ -orthogonal array was applied to the experimental data and the signal-to-noise ratios (SNR) for each level of extraction parameters were measured. The SN-ratio for all responses were combined using the grey relational analysis (GRA) as reported by Kapadiya and Desai (2017). The GRA was used in the determination of optimum extraction condition. Irrespective of the category of quality characteristics, a larger SNR value indicates a better quality characteristics (Abdurahman and Olalere, 2016). The analysis of mean (ANOM) was thereafter conducted to assess the significance of each extraction parameters on the responses (extraction yield (y) and absorbed energy (Q)). The three operating levels of extraction factors were used to design the  $L_9$  orthogonal experimental matrix as shown in Table 1.

### 2.4.2. Validation of optimized condition

The statistical model was validated with respect to the three parameters within the orthogonal array. The experimental results obtained from the point prediction feature (i.e. SN-ratio) in Minitab 17<sup>®</sup> software were compared with the predicted values and the Chi square ( $X^2$ ) values computed in order to determine the significance of the results obtained.

### 2.4.3. Artificial neural network (ANN)

In this study, a feed forward backpropagation multi-layer model was developed using Matlab R2014a (The Mathworks Inc., Ver. 8.3, U.S.A.). The results from parametric study and orthogonal experimental design were used to develop the artificial neural network. Three extraction parameters (extraction time (A), particle size (B) and feed-solvent ratio (C)) were considered as the input layer. The extraction yield and the heat energy absorbed by the water-pepper system were selected as the output layer. For the course of this research, two multilayer resilient backpropagation algorithms (Gradient Descent and Levenberg Marquardt) were employed with log-sigmoid transfer function. The purpose of using the two training algorithms was to prove the strength and ability of the ANN model in predicting similar data instead of going to the lab to conduct the experiments. The algorithm which gives optimum neurons is then selected as the best configuration for subsequent prediction of familiar data. An optimum neurons is obtained from an algorithm with a minimum root mean squared error (RMSE) and highest regression coefficient ( $R^2$ ) (Kapadiya and Desai, 2017). The training was successively conducted until a low root mean square error was obtained for each case of response variable. The network architecture was made of a 60-20-20 framework which has 60% of the data for training, 20% testing and 20% for validation. Data division was made to be by random division to avoid biasness. Data normalization was carried out with a 'mapminmax' algorithm in order to prevent data with high value over-riding those with smaller ones. Optimum neurons were retrieved to obtain minimum root mean squared error and the highest regression coefficient (Thakker et al., 2016).

#### 2.4.4. Data verification in neural network

From the two training algorithms, the estimation of error between actual and predicted output is required for a proper model prediction in artificial neural network (Betiku and Taiwo, 2015). The mean squared error, root mean squared error and regression coefficients are important measures for an effective model prediction in neural network as shown in Eqs. (4) and (5) (Chen, 2008).

$$MSE = \frac{1}{n} \sum_{i=1}^n (y_i - y_{ai})^2 \quad (4)$$

$$RMSE = \sqrt{\frac{1}{n} \sum_{i=1}^n (y_i - y_{ai})^2} \quad (5)$$

where,  $n$  is the number of points,  $y_i$  is the predicted value obtained from the neural network model,  $y_{ai}$  is the actual value.

The overall regression coefficient ( $R^2$ ) gives the evidence of model fitness Eq. (6) (Nath and Chattopadhyay, 2007). The closeness the  $R^2$  value to unity, the better the model fitness into the actual data (Hamid, 2006).

$$R^2 = 1 - \frac{\sum_{i=1}^n \left( \frac{(y_i - y_{ai})^2}{(y_{ai} - y_{ai(ave)})^2} \right)}{n} \quad (6)$$

where,  $n$  is the number of points,  $y_i$  is the predicted value obtained from the neural network model,  $y_{ai}$  is the actual value, and  $y_{ai(ave)}$  is the average of the actual values. Optimum neurons were retrieved to obtain minimum root mean squared error and the highest regression coefficient (Chen, 2008; Harbor, 2013; Thakker et al., 2016). The algorithm which gave the best RMSE and  $R^2$ -value was chosen for further similar problem solving.

### 2.5. Physicochemical characterization

#### 2.5.1. GC-MS analysis

Gas Chromatography-Mass Spectrometry analysis was conducted to determine the chemical constituents in the extracts. An Agilent GC-MS instrument (5975C inert, USA) equipped with mass spectrometer (MS) was used alongside with a GC system (Agilent 7890A). A C-18 column of tubular diameter of 30 mm, internal diameter of 0.25 mm, and a film thickness of 0.25  $\mu$ m was employed. The column initial oven hold was operated at 50 °C for 5 min and then allowed to rise to 250 °C at 3 °C per min. The micro-filtered samples were diluted with analytical grade acetone at a ratio of 1:10 in mL. A 1.0  $\mu$ L of the diluted solution was then injected into the gas chromatography column at 280 °C and a carrier helium gas velocity of 1 ml/min with a total run time of 69 min. The chemical compounds present in the extracts and their quantification were conducted in relation to their retention indices from the National Institute of Standard and Technology, NIST MS library. The percentage compositions were calculated in accordance with the area of each peak (Jeyaratnam et al., 2016).

#### 2.5.2. Scanning electronic microscopy (SEM)

Morphological transformations of the pepper samples after the heat refluxation were investigated through SEM analysis. SEM images of the dried extracts obtained at optimum extraction condition were obtained using the Scanning Electronic Microscope (SEM) (Tabletop Microscope-3030Plus, USA). The test samples were mounted on an adhesive plate, air-dried and coated with thin layer gold before analysis to remove any electrical discharge (Olalere et al., 2017). The raw dried pepper and extracts were subjected to an accelerated voltage of 15 kV and 40-300x magnification with an acquisition time of 30 s.

## 3. Results and discussion

### 3.1. Multi-response optimization

The results obtained from black pepper heat reflux extraction placed the optimum extraction condition at 240 min of extraction time, 0.154 mm of particle size, and 1:14 of feed-solvent ratio. The extraction yield and energy absorbed under the optimum condition were, 13.22 (mg extracts/25 g sample) and 285.60 J/min, respectively. However, in white pepper heat reflux extraction, the optimum extraction condition was attained at 180 min of extraction time, 0.105 mm of particle size of, and 1:18 of feed-solvent ratio. Under this condition, the total extracts and energy absorbed was 14.04 (mg extracts/25 g sample) and 264.82 J/min, respectively. These were the condition at which the extraction parameters jointly optimized the extraction yield and absorbed microwave energy (Table 2). Hence, by using the above conditions, an improved extraction yield is achievable at optimized energy absorption capacity.

### 3.2. Validation of orthogonal design results

The predicted optimal responses were validated using triplicate parallel tests as presented in Table 3. From the optimal yield and absorbed energy ( $y_b = 13.22$  mg/g,  $Q_{tb} = 285.60$  J/min) three confirmatory tests were conducted on the black pepper heat refluxation and the estimated X-goodness-of-fit obtained from the confirmatory tests was 0.014 and 0.042 from extraction yield and absorbed energy, respectively. Similarly, three parallel tests were also conducted from predicted optimal yield and absorbed energy in white pepper heat refluxation ( $y_w = 14.04$  mg/g,  $Q_{tw} = 264.82$  J/min). The estimated X-goodness-of-fit test values from white pepper refluxation were 0.078 and 0.071 for extraction yield and absorbed energy, respectively. In both cases, the X-goodness-of-fit test between the predicted and experimented responses clearly revealed a smaller X-values when compared with the 7.81 cut-off value for a 3-degree of freedom at 95% confidence level (Alara et al., 2019; Olalere et al., 2017; Subroto et al., 2015). This confirmed a no-significant difference between the predicted and actual optimum response values.

### 3.3. Statistical analysis of mean (ANOM)

The average response means, the extremum or delta difference ( $\beta_{max} - \beta_{min}$ ) were computed with  $\beta_{max}$  and  $\beta_{min}$  being the largest and smallest average response means, respectively. The mean effects for each extraction factor were determined using the value generated from their extremum differences. The average means for the extraction yield and absorbed energy are presented in Table 4.

Fig. 1 (a) showed the individualistic effects of each extraction variable on the average yield. The maximum average yield obtained were 10.2 mg/g at level-3 of extraction time (240 min), 9.53 mg/g at level-2 of particle size (0.154 mm), and 9.05 mg/g at level-2 of feed-solvent ratio (1:16). Meanwhile, in Fig. 1 (b), the maximum average absorbed energy were 278.00 J/min at level-3 of extraction time (240 min), 274.60 J/min at level-2 of particle size (0.154 mm), and 276.90 J/min at level-2 of feed-solvent ratio (1:16). The order of contribution of the extraction parameters at different operating levels to the average yield and absorbed energy was  $A > C > B$ . The decreasing order of significance affirmed extraction time as the largest contributor to spice oleoresin extraction from black pepper. The higher time requirement in black pepper heat reflux could be attributed to the higher inter-molecular forces of attraction between their parenchymatous cells (Olalere et al., 2017). This indicated that the production of black pepper from

**Table 2**Experimental layout using  $L_9$  orthogonal array and the responses.

Exp. no	Independent variables			Responses from black pepper		Responses from white pepper	
	A	B	C	$y_b^a$ (mg/g)	$Q_t b^a$ (J/min)	$y_w^a$ (mg/g)	$Q_t w^a$ (J/min)
1	1	1	1	6.14 ± 0.34	228.00 ± 0.07	10.05 ± 0.09	225.15 ± 0.05
2	1	2	2	8.17 ± 0.41	274.04 ± 0.13	12.13 ± 0.15	257.73 ± 0.24
3	1	3	3	5.96 ± 0.03	255.86 ± 0.34	8.66 ± 0.32	162.10 ± 0.18
4	2	1	2	9.42 ± 0.16	275.88 ± 0.04	14.04 ± 0.25	264.82 ± 0.44
5	2	2	3	7.20 ± 0.01	264.03 ± 0.10	11.91 ± 0.01	246.44 ± 0.36
6	2	3	1	6.93 ± 0.22	259.58 ± 0.06	9.74 ± 0.02	213.19 ± 0.03
7	3	1	3	7.81 ± 0.10	267.63 ± 0.19	10.59 ± 0.32	244.48 ± 0.10
8	3	2	1	13.22 ± 0.11	285.60 ± 0.45	10.39 ± 0.04	238.81 ± 0.27
9	3	3	2	9.57 ± 0.03	280.67 ± 0.03	10.50 ± 0.01	239.48 ± 0.01

<sup>a</sup> Values are means ± SD of triplicate runs.**Table 3**

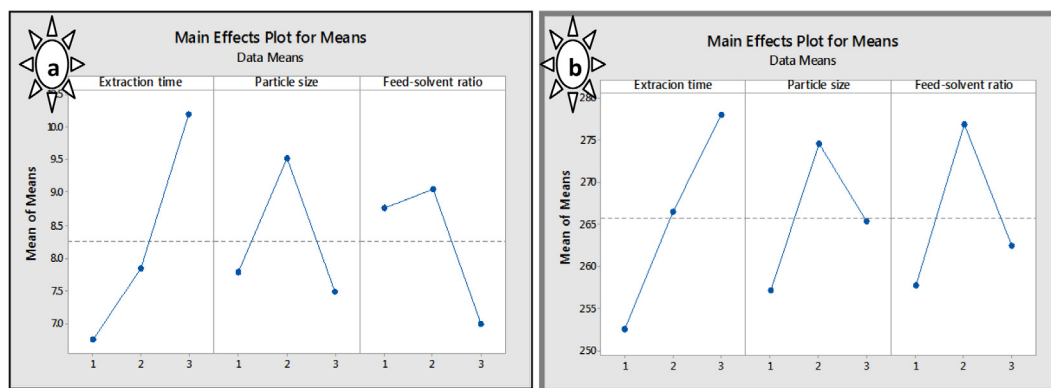
Results of parallel tests.

Run	Experimental extraction yield (mg/g)		Experimental absorbed energy (J/min)	
	Black pepper fixed oil	White pepper fixed oil	Black pepper fixed oil	White pepper fixed oil
1	13.25	14.02	284.89	263.67
2	13.21	14.03	285.65	264.65
3	13.18	13.75	285.60	264.83

**Table 4**

Average mean effects.

	Average responses for black pepper heat refluxation						Average responses for white pepper heat refluxation					
	$y_{b(av)}$ (mg/g)			$Q_{b(av)}$ (J/min)			$y_{w(av)}$ (mg/g)			$Q_{w(av)}$ (J/min)		
	A	B	C	A	B	C	A	B	C	A	B	C
$\beta_{i_1}$	6.8	7.8	8.8	252.6	257.2	257.7	10.3	11.6	10.0	215.0	244.8	225.7
$\beta_{i_2}$	7.9	9.5	9.0	266.5	274.6	276.9	11.9	11.5	12.2	241.5	247.7	254.0
$\beta_{i_3}$	10.2	7.5	7.0	278.0	265.4	262.5	10.5	9.6	10.4	240.9	204.9	217.7
D	3.4	2.0	2.1	25.3	17.4	19.1	1.6	1.9	2.2	26.5	42.7	36.3
%D	45 <sup>a</sup>	27	28	41 <sup>a</sup>	28	31	28	33	39 <sup>a</sup>	25	40 <sup>a</sup>	34

<sup>a</sup> Highest contributors to the response mean.**Fig. 1.** Average mean effects-black pepper (a) average yield black pepper (b) average energy black pepper.

an immature peppercorn has effect on the time requirement during the heat reflux extraction (Zaveri et al., 2010). However, particle size has the least effects on the extraction yield and energy absorbed in the heat reflux extraction of black pepper.

In white pepper heat refluxation, the maximum average yield was 11.90 mg/g at level-2 of extraction time (180 min), 11.56 mg/g at level-1 of particle size (0.105 mm), and 12.22 mg/g at level-2 of feed-solvent ratio (1:16) as illustrated in Fig. 2(a). Furthermore, maximum average energy absorbed was 241.50 J/min at level-2 of extraction time (180 min), 247.70 J/min at level-2 of par-

ticle size (0.154 mm), and 254.00 J/min at level-2 of feed-solvent ratio (1:16) as shown in Fig. 2(b). The extraction factor with the highest extremum difference was declared as having the most contributing effect on the response settings (Abbass et al., 2016). In this case, the feed-solvent ratio gave the highest contribution to the extraction yield and absorbed energy. The extracting solvent (water) therefore provided a good interaction with the pepper matrix with a decreasing order of  $C > A > B$ . A threshold solvent volume of 400 ml provided a strong interaction between the solvent and pepper sample (Olalere et al., 2017; Olawale, 2012). The



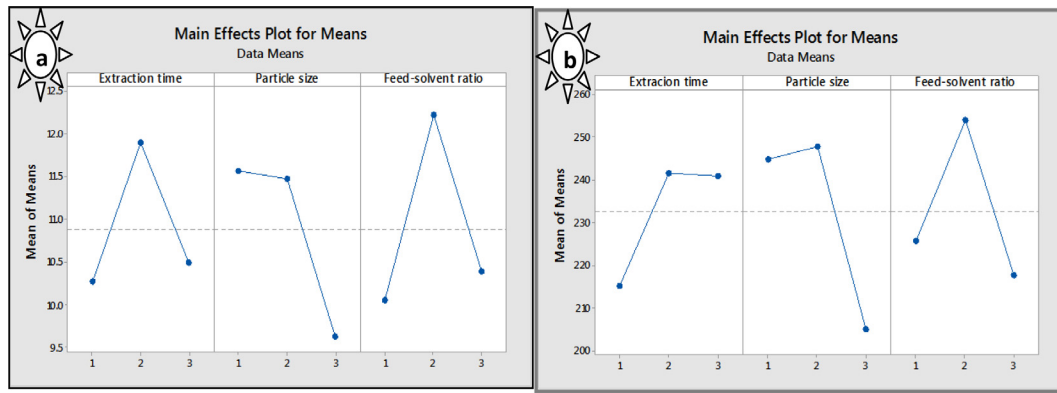


Fig. 2. Average mean effects-white pepper (a) average yield white pepper (b) average energy white pepper.

result therefore indicated that feed-to-solvent ratio (C) has the most significant contribution to the extraction of fixed oil from white pepper. However, the particle size has the least contribution to the extraction yield and energy absorbed by white pepper in heat reflux extraction.

### 3.4. ANN prediction

In the ANN model prediction, the network inputs were the extraction time (A), particle size (B) and feed-solvent ratio (C). The extraction yield and absorbed energy are the output variable in black and white heat reflux extraction. The Gradient Descent and Levenberg–Marquardt training algorithms were hidden layers used in conjunction with tansigmoid transfer function. The 3–4–5–1 topology was employed and this signifies that the model has 3 input layers, 4 neurons in the first hidden layer, 5 neurons in the second hidden layer and one output layer. The networks were trained severally for each response variable until both the coefficient of regression for training and prediction (between the simulated responses and expected responses) increases.

#### 3.4.1. ANN prediction using Gradient Descent algorithm

The overall regression coefficient of 0.9370 and root mean squared error of 0.8849 was obtained for the optimum yield from black pepper. While an overall regression coefficient and root mean squared error of 0.9387 and 0.2565 were generated for the optimum yield from white pepper. Similarly, the overall regression coefficient and root mean squared error was 0.9959 and 0.7725 for optimal energy absorbed in black pepper heat reflux. Whereas, for the optimum yield in white pepper heat reflux, the overall regression coefficient and root mean squared error was 0.9114 and 0.3206 respectively. The result shows a good agreement with the optimality of Taguchi experimental design data as presented in Table 5.

Fig. 3 is the post regression plot of predicted results and the expected trained network response. The primary aim of training and retraining the network is to provide a better function approximation which can enable it predict similar problem (Aggarwal, 2015). The regression value for the training process must therefore

be closer to unity ( $\approx 1$ ) for a better prediction. For this study, the higher regression coefficients obtained between the network outputs is an indication of good training in the supervised neural learning process neural network. Moreover, the root mean square error obtained from the training process went through a marginal reduction as the number of iterations was increased. The smaller MSE and RMSE values further validated a good training and better prediction (Thakker et al., 2016).

#### 3.4.2. ANN prediction using Levenberg–Marquardt training algorithm

Table 6 is the results obtained from ANN prediction per input variable using Levenberg–Marquardt training algorithm. The overall regression coefficient and root mean squared error of 0.9551 and 0.5701 respectively were generated from optimum yield in black pepper heat refluxation. While an overall regression coefficient and root mean squared error of 0.9845 and 0.5708 respectively for optimum yield in white pepper heat refluxation. Similarly the overall regression coefficient and root mean squared error was 0.9398 and 0.7258 for optimal energy absorbed in black pepper heat refluxation. Whereas for the optimum yield in white pepper heat refluxation, the overall regression coefficient and root mean squared error was 0.9546 and 0.4525 respectively. The summary of the overall regression coefficient and root mean squared error for each response in black and white pepper heat refluxation. Table 6 consists of results obtained from the Levenberg–Marquardt algorithm.

Fig. 4 is the post regression analysis with a comparison between the predicted experimental results and the expected. The results obtained gave regression values closer to unity ( $\approx 1$ ) and lower root mean square errors. The proximity of the regression coefficient and lower root mean square errors showed good training and a better prediction.

#### 3.4.3. Comparison between results obtained from GD and LM algorithm

On the overall, the Levenberg–Marquardt (LM) training algorithm gave a faster convergence during the training process compared with the Gradient Descent (GD) method. Hence, less iteration is necessary before one of the convergence criteria was

Table 5  
Network training configuration and results (Gradient Descent).

Sample name	Output	Transfer function	Model topology	MSE	RMSE	R <sup>2</sup>
Black pepper	y <sub>b</sub>	tansig	3–4–5–1	0.7831	0.8849	0.9370
	Q <sub>tb</sub>	tansig	3–4–5–1	0.5968	0.7725	0.9959
White pepper	y <sub>w</sub>	tansig	3–4–5–1	0.0658	0.2565	0.9387
	Q <sub>tw</sub>	tansig	3–4–5–1	0.1028	0.3206	0.9114

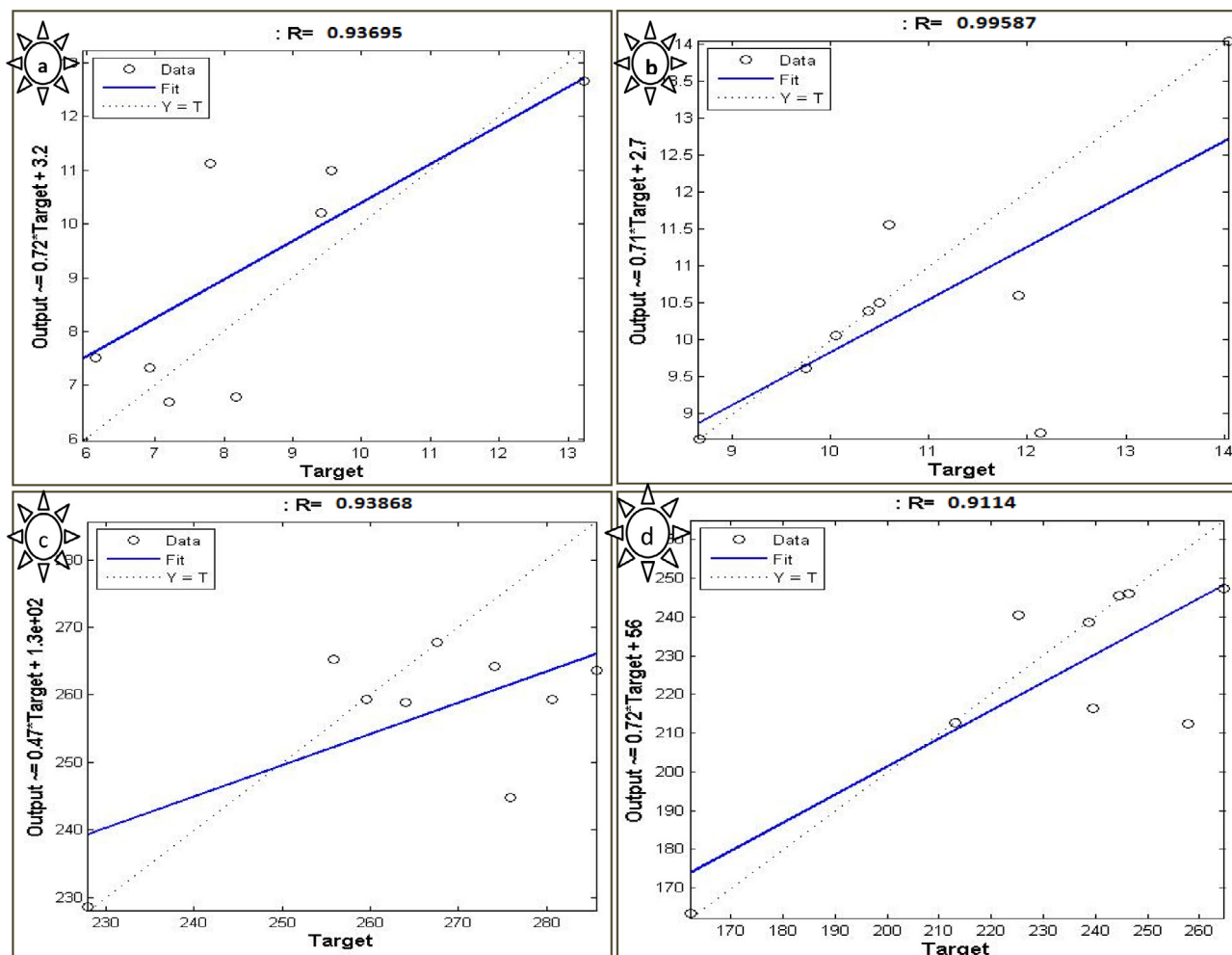


**Fig. 3.** Post regression analysis with Gradient Descent algorithm (a) average yield black pepper (b) average energy black pepper (c) average yield white pepper (d) average energy white pepper.

**Table 6**  
Network training configuration and results (Levenberg-Marquardt).

Sample name	Output	Transfer function	Model topology	MSE	RMSE	R <sup>2</sup>
Black pepper	y <sub>b</sub>	tansig	3-4-5-1	0.3250	0.5701	0.9551
	Q <sub>tb</sub>	tansig	3-4-5-1	0.5268	0.7258	0.9398
White pepper	y <sub>w</sub>	tansig	3-4-5-1	0.3258	0.5708	0.9845
	Q <sub>tw</sub>	tansig	3-4-5-1	0.2048	0.4525	0.9546

reached. The LM- algorithm can therefore be saved and the network from the parametric data retrained to get better result. However, care must be taken to prevent over-fitting which might results in poor function generalization when dealing with new parametric data.

### 3.5. Chemical composition

The relative abundance of each classes of compound identified from GC-MS analysis of the black (BPOE) and white (WPOE) extracts are presented in Fig. 5. A total of 19 components were identified in GC-MS analysis of BPOE and the major components were piperine (37.85%), caryophyllene (8.97%), sabinene (5.76%), limonene (4.51%), and  $\beta$ -bisabolene (1.66%). Moreover, the extracted oleoresin consisted of 39.38% alkaloids, 11.06% monoterpenes hydrocarbons, 2.23% oxygenated monoterpenes and 13.19%

sesquiterpenes. These suggested that the alkaloids have the highest concentration of bioactive compounds, followed by monoterpenes and sesquiterpenes. Moreover,  $\alpha$ -Thujene, guineensine, 1-cinnamoyl piperidine, piperettine,  $\alpha$ -selinene,  $\alpha$ -cubebene were found to be in trace amount as reported by Singh et al. (2013). However, in WPOE a total of 25 bioactive compounds were identified with piperine (42.29%), caryophyllene (10.36%), sabinene (7.94%), limonene (6.47%), and  $\beta$ -bisabolene (2.42%) as major components. The white pepper extract contained 44.36% of alkaloids, 16.21% of monoterpenes hydrocarbons, 3.97% of oxygenated monoterpenes, and 14.03% of sesquiterpenes. The higher concentration of compounds such as piperine, caryophyllene, sabinene, limonene and  $\beta$ -bisabolene in white pepper oleoresin extracts (WPOE) is therefore an indication of its higher nutritional and functional characteristics than black pepper oleoresin extracts (BPOE) as illustrated in Fig. 5.

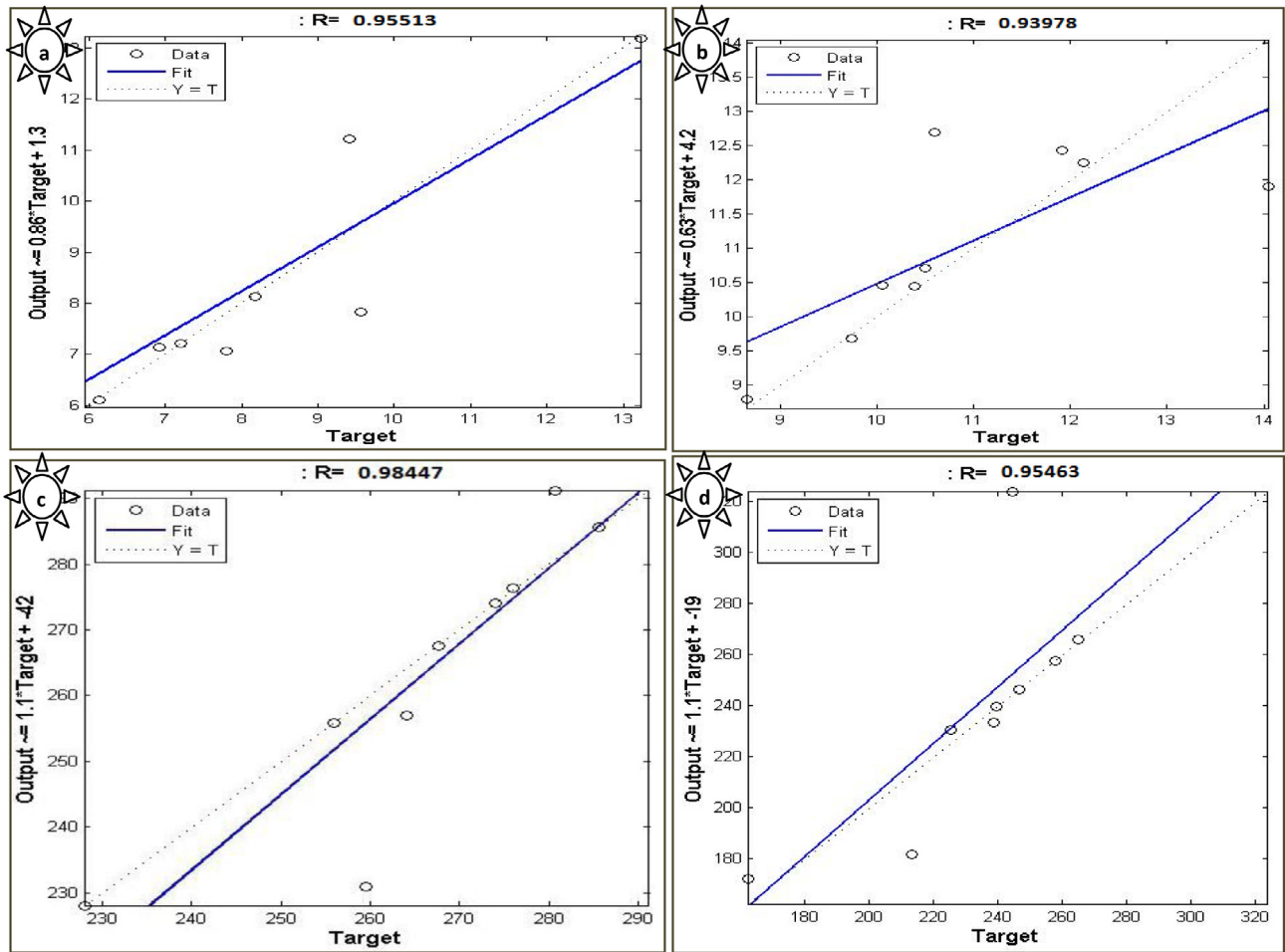


Fig. 4. Post Regression analysis with Levenberg Marquardt algorithm (a) average yield black pepper (b) average energy black pepper (c) average yield white pepper (d) average energy white pepper.

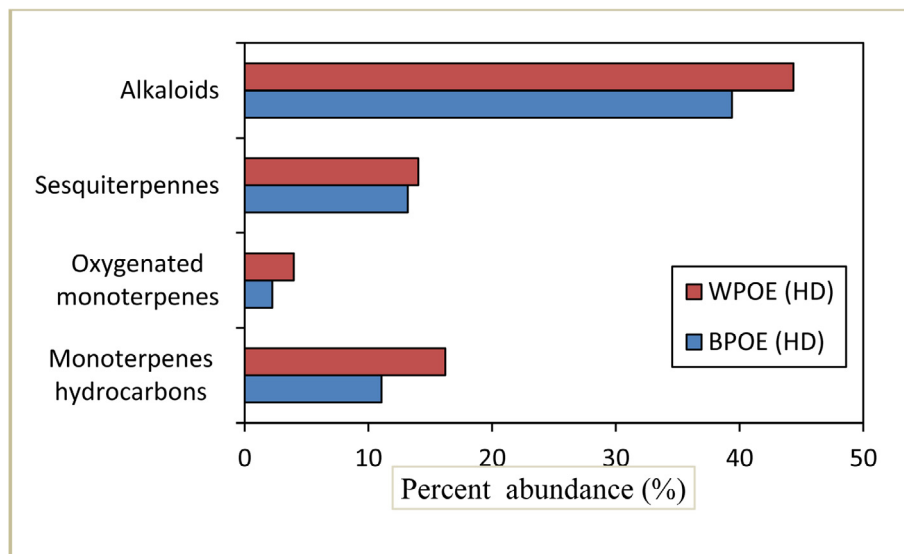
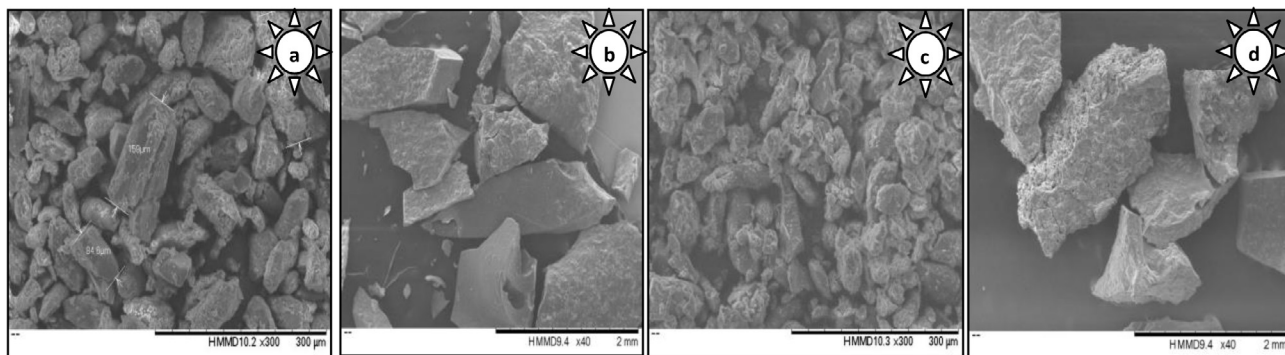


Fig. 5. Percentages of different classes of compounds extracted from black and white pepper.

### 3.6. Morphological characteristics

The medullary and peripheral bundles are the two striking features in the structure of black and white pepper (Ravindran, 2000).

It composed of layer of stone like elongated parenchymatous cells which are neatly packed in a fresh sample as shown in Fig. 6 (a) and (c). The cellulosic cell wall of an untreated fresh pepper sample first experienced an induction process in which the outer vascular



**Fig. 6.** SEM-monograph (a) Black *P.nigrum* at pre-extraction (b) Black *P.nigrum* at post-extraction (c) White *P.nigrum* at pre-extraction (d) White *P.nigrum* at post-extraction heating.

bundles swell due to the penetration effect of solvent. As a result of the localized heating effects on the pepper matrix, the membrane structure of the cellulose cell wall becomes disoriented thereby resulting in a subsequent rupture. The elongated stone like cells then become broken into smaller forms which lead to a reduced surface area. Fig. 6 (a) and (c) the ordered thin-wall stone-like elongated cells of fresh black and white pepper, respectively. Fig. 6 (b) and (d) are the ruptured cells after exposure of white pepper to the conventional localized heat.

#### 4. Conclusion

In this study, the extracts from black and white pepper were optimized using the Taguchi orthogonal design of experiment. This design investigated the effects of three independent variables (extraction time, particle size, and feed-solvent ratio) on the yield and absorbed energy. In the black pepper reflux extraction, the optimal extraction yield and energy absorbed under the optimum condition were 13.22 (mg extracts/25 g sample) and 285.60 J/min, respectively. Moreover, in white pepper heat refluxation, the optimal extraction yield and energy absorbed under the optimum condition were 14.04 (mg extracts/25 g sample) and 264.82 J/min, respectively. Artificial neural network was used for intelligent prediction, using the results from Taguchi experimental design. Two algorithms were compared and better prediction of the experimental data were obtained from the Levenberg Marquardt with tanlog sigmoid transfer function as hidden layer and 3-4-5-1 as model topology. Hence the Levenberg Marquardt feed forward backpropagation model is a viable tool to optimally predict result for different combination of operating variables in extraction process.

#### Conflicts of interest

All contributing authors declare no conflicts of interest.

#### Acknowledgements

Our gratitude also goes to the Research and Innovation Department, Universiti Malaysia Pahang, Malaysia, for their support through the PGRS-160320 research grant.

#### References

Abbass, M.K., Hussein, S.K., Khudhair, A.A., 2016. Optimization of mechanical properties of friction stir spot welded joints for dissimilar aluminum alloys (AA2024-T3 and AA 5754-H114). *Arab. J. Sci. Eng.* <http://dx.doi.org/10.1007/s13369-016-2172-9>.

Abdurahman, N.H., Olalere, O.A., 2016. Taguchi-based based optimization technique in reflux microwave extraction of piperine from black pepper (*Piper nigrum*). *Aust. J. Basic App. Sci.* 10, 293–299.

Adedeji, P.A., Olalere, O.A., Adebimpe, O.A., Olanusi, S., 2014. Neural network based user interface for accident forecast in manufacturing industries. *Int. J. Eng. Sci.* 73–79.

Aggarwal, R., 2015. Effect of training functions of Artificial Neural Networks (ANN) on time series forecasting. *Int. J. Computer App.* 109, 14–17.

Alara, O.R., Abdurahman, N.H., Abdul Mudalip, S.K., Olalere, O.A., 2019. Effects of drying on free radicals scavenging and chemical compositions of vernonia amygdalina leaf extracts growing in Malaysia. *J. King Saud Univ. Sci.* 31, 495–499. <http://dx.doi.org/10.1016/j.jksus.2017.05.018>.

Betiku, E., Taiwo, A.E., 2015. Modeling and optimization of bioethanol production from breadfruit starch hydrolyzate. *Renew. Energy* 74, 87–94. <http://dx.doi.org/10.1016/j.renene.2014.07.054>.

Chen, L.J., 2008. Integrated Robust Design Using Response Surface Methodology and Constrained Optimization. *Response. Syst. Des. Eng.* University of Waterloo.

Nath, A., Chattopadhyay, P.K., 2007. Optimization of oven toasting for improving crispness and other quality attributes of ready to eat potato-soy snack using response surface methodology. *J. Food Eng.* 1282–1292. <http://dx.doi.org/10.1016/j.jfoodeng.2006.09.023>.

Gavahian, M., Farahnaky, A., Farhoosh, R., Javidnia, K., Shahidi, F., 2015. Extraction of essential oils from *Mentha piperita* using advanced techniques: microwave versus ohmic assisted hydrodistillation. *Food Bioprod. Process.* 94, 50–58. <http://dx.doi.org/10.1016/j.fbp.2015.01.003>.

Hamid, N., 2006. Optimization of enzymatic clarification of sapidilla juice using response surface methodology optimization of enzymatic clarification of sapidilla juice using response surface methodology. *J. Food Eng.* 73, 13–319. <http://dx.doi.org/10.1016/j.jfoodeng.2005.01.031>.

Harbor, D., 2013. Computers & geosciences neuro-fuzzy and neural network techniques for forecasting sea level. *Comput. Geosci.* 52, 50–59. <http://dx.doi.org/10.1016/j.cageo.2012.09.015>.

Jagella, T., Grosch, W., 1999. Flavour and off-flavour compounds of black and white pepper (*Piper nigrum* L.). I. Evaluation of potent odorants of black pepper by dilution and concentration techniques. *Eur. Food Res. Technol.* 209, 16–21.

Janakiraman, K., Manavalan, R., 2008. Studies on effect of piperine on oral bioavailability of ampicillin and norfloxacin. *Afr. J. Tradit. Complement Altern. Med.* 5, 257–262.

Jeyaratnam, N., Nour, A.H., Kanthasamy, R., Nour, A.H., Yuvaraj, A.R., Akindoyo, J.O., 2016. Essential oil from *Cinnamomum cassia* bark through hydrodistillation and advanced microwave assisted hydrodistillation. *Ind. Crops Prod.* 92, 57–66. <http://dx.doi.org/10.1016/j.indcrop.2016.07.049>.

Kapadiya, S., Desai, M.A., 2017. Isolation of essential oil from buds of *syzygium aromaticum* using hydrodistillation: multi-response optimization and predictive modelling. *Int. J. Adv. Res. Sci Eng.* 6, 405–418.

Mandal, V., Mohan, Y., Hemalatha, S., 2008. Microwave assisted extraction of curcumin by sample-solvent dual heating mechanism using Taguchi L9 orthogonal design. *J. Pharm. Biomed. Anal.* 46. <http://dx.doi.org/10.1016/j.jpba.2007.10.020>.

Mohan, M., Khanam, S., Shivananda, B.G., 2013. Optimization of microwave assisted extraction of andrographolide from *andrographis paniculata* and its comparison with refluxation extraction method. *Res. Article* 2, 342–348.

Olalere, O.A., Abdurahman, N.H., Alara, O.R., Habeeb, O.A., 2017. Parametric optimization of microwave reflux extraction of spice oleoresin from white pepper (*Piper nigrum*). *J. Anal. Sci. Technol.* 8, 8. <http://dx.doi.org/10.1186/s40543-017-0118-9>.

Olawale, A.S., 2012. Solid-liquid extraction of oils of African elemi's (*Canarium schweinfurthii*'s) fruit. *Agric. Eng. Int. CIGR J.* 14, 155–160.

Raman, G., Gaikar, V., 2002. Microwave-assisted extraction of piperine from *Piper nigrum*. *Ind. Eng. Chem. Res.* 41, 2521–2528. <http://dx.doi.org/10.1021/ie010359b>.

Ravindran, P., 2000. Black Pepper, *Piper Nigrum*.



- Reshmi, S.K., Sathya, E., Devi, P.S., 2010. Isolation of piperidine from *Piper nigrum* and its antiproliferative activity. *African J. Pharm. Pharmacol.* 4, 562–573. <http://dx.doi.org/10.5897/JMPR10.033>.
- Sahin, S., Samli, R., Tan, A.S.B., Barba, F.J., Chemat, F., Cravotto, G., Lorenzo, J.M., 2017. Solvent-free microwave-assisted extraction of polyphenols from olive tree leaves: antioxidant and antimicrobial properties. *Molecules* 22, 1056. <http://dx.doi.org/10.3390/molecules22071056>.
- Şahin, S., Sayim, E., Samli, R., 2017. Comparative study of modeling the stability improvement of sunflower oil with olive leaf extract. *Korean J. Chem. Eng.* 34, 2284–2292. <http://dx.doi.org/10.1007/s11814-017-0106-1>.
- Scott, I.M., Jensen, H.R., Philogène, B.J.R., Arnason, J.T., 2007. A review of *Piper* spp. (Piperaceae) phytochemistry, insecticidal activity and mode of action. *Phytochem. Rev.* 7, 65–75. <http://dx.doi.org/10.1007/s11101-006-9058-5>.
- Shahida, M.S., Abdul Majid, F.A., Wan Mustapha, W.A., Jantan, I., 2013. Anti-inflammatory activity of selected edible herbs and spices on cultured human gingival fibroblasts. *Open Conf. Proc. J.* 4, 33–37. <http://dx.doi.org/10.2174/2210289201304010236>.
- Singh, S., Kapoor, I.P.S., Singh, G., Schuff, C., De Lampasona, M.P., Catalan, C.A.N., 2013. Chemistry, antioxidant and antimicrobial potentials of white pepper (*Piper nigrum* L.) essential oil and oleoresins. *Proc. Natl. Acad. Sci. India Sect. B – Biol. Sci.* 83, 357–366. <http://dx.doi.org/10.1007/s40011-012-0148-4>.
- Subroto, E., Manurung, R., Heeres, H.J., Broekhuis, A.A., 2015. Optimization of mechanical oil extraction from *Jatropha curcas* L. kernel using response surface method. *Ind. Crops Prod.* 63, 294–302. <http://dx.doi.org/10.1016/j.indcrop.2014.08.050>.
- Thakker, M.R., Parikh, J.K., Desai, M.A., 2016. Microwave assisted extraction of essential oil from the leaves of *Palmarosa*: multi-response optimization and predictive modelling. *Ind. Crops Prod.* 86, 311–319. <http://dx.doi.org/10.1016/j.indcrop.2016.03.055>.
- Toboc, A., Lavric, V., 2012. Artificial neural network modelling of ultrasound and microwave extraction of bioactive constituents from medicinal plants. *Plants. Rev. Chim.*, 63.
- Zaveri, M., Khandhar, A., Patel, S., Patel, A., 2010. Chemistry and pharmacology of *Piper longum* L. *Int. J. Pharm. Sci. Rev. Res.* 5, 67–76.